INSOLUBLE ORGANIC MATTER IN RYUGU ANALOG METEORITE JBILET WINSELWAN. B. T. De Gregorio[1] and R. M. Stroud[1], [1]U.S. Naval Research Laboratory (4555 Overlook Ave. SW, Code 6366, Washington, DC 20375; bradley.degregorio@nrl.navy.mil).

Introduction: The JAXA Hayabusa2 mission successfully returned the first pristine samples of a C-type asteroid (162173 Ryugu) to Earth for laboratory analysis on December 6th, 2020. Carbonaceous matter located within these returned regolith grains will provide a unique opportunity to study chondritic organic matter in the absence of potential alteration by atmospheric reentry heating or terrestrial contamination.

The shape and intensity of the global 2.7 μm feature from NIR measurements of the Ryugu surface are consistent with that of shocked or heated CM meteorites [1]. For this reason, we selected the thermally altered CM2 chondrite Jbilet Winselwan [2] as an analog. The chemical functionality, composition, and distribution of insoluble organic matter (IOM) in this analog meteorite will give insight into the nature of IOM on Ryugu.

Methods: Because many of the regolith grains collected by Hayabusa2 are >10^2 μm, based on touchdown videos, sample canister images, and high thermal inertia values [3], standard ultramicrotomy techniques will not be optimal for their processing. Here, we used a hybrid approach, combining focused ion beam (FIB) milling with ultramicrotomy, similar to that described in [4]. We extracted a 15 x 15 μm "chunk" was extracted from a ~350 μm particle of crushed Jbilet Winselwan matrix with a FEI Helios G3

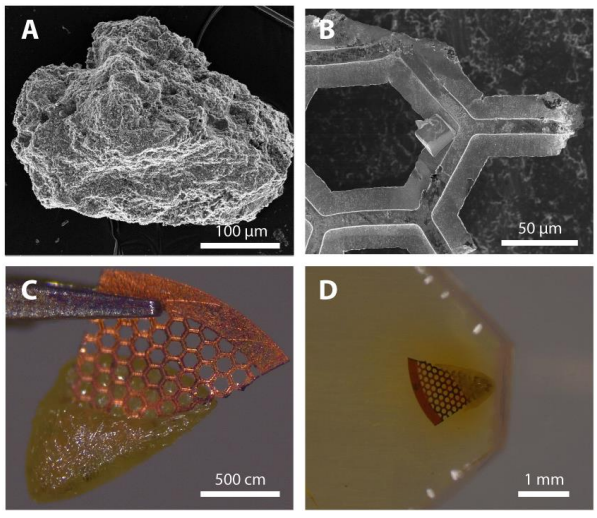

Figure 1. (A) Secondary electron (SE) image of Jbilet Winselwan matrix particle. (B) SE image of extracted chunk after placement on cut grid. (C) Cut grid after coating in S. (D) Final double-embedded sample.

FIB-SEM and attached it to the tip of a wedge-cut Cu TEM grid (Figure 1). The tip of this cut grid was coated in S, embedded in epoxy, and ultramicrotomed (70 nm). Sections of the particle chunk and grid were placed on Cu TEM grids with a lacey C support film. For comparison, a standard FIB liftout section was prepared from another matrix particle.

Scanning-transmission X-ray microscopy (STXM) was performed on beamline 5.3.2.2 at the Advanced Light Source. X-ray absorption near-edge structure (XANES) datasets were collected at the C and N absorption edges to locate IOM within the sample and measure its organic functional chemistry at a spatial resolution of ~35 nm. Subsequent scanning-transmission electron microscopy (STEM) was performed with the Nion UltraSTEM-X at NRL. The STEM analysis was performed at 60 keV to minimize beam damage to C, N, and O bonds, although some H loss cannot be avoided. Simultaneous electron energy-loss spectroscopy (EELS) and energy dispersive X-ray spectroscopy (EDS) datasets were collected at a 20 nm spatial resolution for comparison with XANES data.

Results: *STXM-XANES.* Carbonaceous matter is sparse in both Jbilet Winselwan samples, with only a handful of dense IOM grains observed in C absorption images. These IOM grains have similar organic chemical functionality as other CM chondrite IOM (such as Murchison), dominated by aromatic (C=C; 285 eV), ketone (C=O, 286.5 eV), and carboxyl (COOH; 288.5 eV) X-ray absorption peaks (Figure 2). However, the aromatic peak for Jbilet Winselwan IOM shows a ~50% increase over Murchison IOM, consistent with the general growth of polyaromatic domains from an increased level of parent body heating. No N absorption was detected, consistent with an average N/C of ~1 at.% or less. Similar results were obtained from IOM within the FIB-prepared section.

STEM-EELS-EDS. Despite having a low N content, STEM-EDS mapping of IOM in Jbilet Winselwan detects a variation in N/C of 0.01-0.05 within a single IOM grain (Figure 3). This variation corresponds to subtle changes in EELS spectra (Figure 3D). Specifically, the presence of higher N is associated with a shift of the main C=C absorption to 285.5 eV, most likely due to a greater abundance aromatic C=N in pyrrole and pyridine functional groups [6]. EDS mapping also reveals an unexpected S enrichment (~0.5 at.%) in the IOM (Figure 3C). This amount of S (which is simultaneously absent from the surrounding

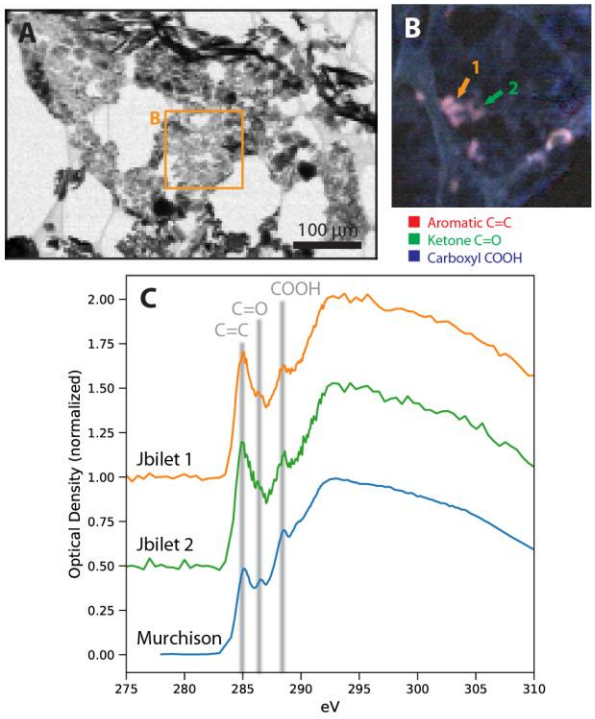

Figure 2. (A) STXM image of Jbilet Winselwan section. (B) False-color RGB image of X-ray absorption of three major organic functional groups. (C) C-XANES spectra of two IOM grains, compared with average Murchison IOM [5].

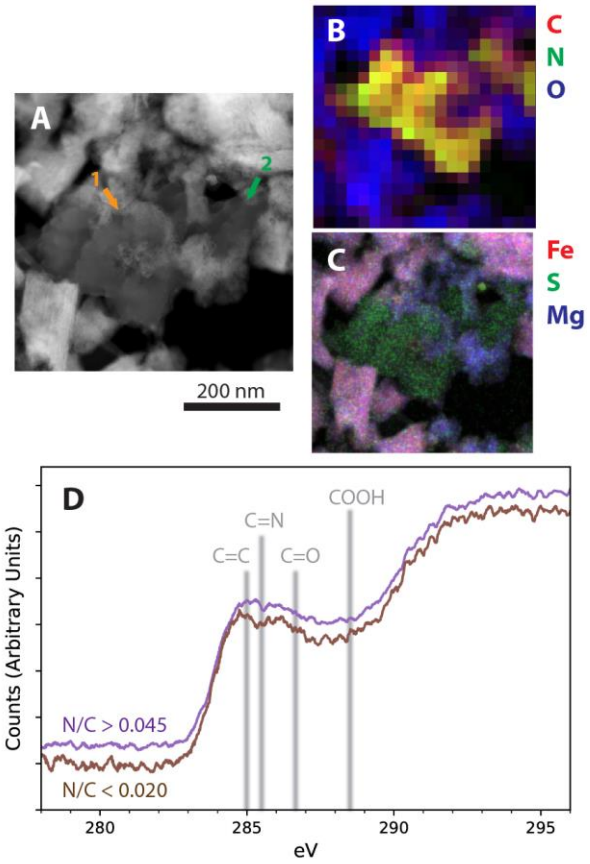

Figure 3. (B) STEM image of the same IOM grains shown in Figure 2. (B,C) False-color EDS maps showing composition of IOM and surrounding inorganic materials. Map (B) was acquired simultaneously with EELS at the same 20 nm/pixel spatial resolution. (D) Summed C-EELS spectra of high N and low N IOM from grain #1.

material) is inconsistent with S incorporation during S embedding, but is likely indigenous to the IOM.

Discussion: Recent *in situ* research on IOM in carbonaceous chondrites has noted an intimate relationship between IOM and amorphous silicates/phyllosilicates (e.g., [7-8]). In Jbilet Winselwan, the particulate IOM shown in Figure 3A is interspersed with a Fe-poor disordered silicate material (Si+Al/Fe+Mg ~ 1.2). Reaction with sulfur-bearing amorphous silicates during hydrothermal parent body alteration could also be responsible for the observed S enrichment in the IOM. Both the XANES and EELS data indicate a greater abundance of aromatic carbon than typically found in primitive CM chondrites (Figure 2C), consistent with the elevated thermal history of Jbilet Winselwan.

The combination of STXM-XANES and STEM-EELS-EDS provides an information-rich dataset from which to gain insight and interpret the origin of IOM in meteorite and asteroid samples. Even in a heated meteorite like Jbilet Winselwan, where non-C heteroatoms typically have a low abundance, slight variations in organic functional group diversity can be tracked at the nm scale. The analytical approach detailed here will later be applied to returned samples from Ryugu.

Acknowledgments: This work was funded by NASA awards 80HQTR20T0050 and 80NSSC19M0215. The ALS beamline is supported by the U.S. DOE Office of Science (contract DE-AC02-05CH11231).

References: [1] Kitazato K. et al. (2019) Science, 364, 272-275. [2] King A. J. et al. (2019) Meteoritics & Planet. Sci., 54, 521-543. [3] Grott M. et al. (2019) LPSC L, abstract #1267. [4] Ohtaki K. et al. (2020) Microscopy & Microanalysis, 26, 120-125. [5] De Gregorio B. T. et al. (2010) GCA, 74, 4454-4470. [6] Latham K. G. et al. (2018) Carbon, 128, 179-190. [7] Le Guillou C. et al. (2014) GCA, 131, 368-392. [8] Vinogradoff V. et al. (2017) GCA, 212, 234-252.